Profiles and springs optimization in a VVA distribution system for internal combustion engines

ALERAMO LUCIFREDI, AMEDEO RONCALLO, PAOLO SILVESTRI
Lab. MGMV-Department of Mechanics
University of Genova
Via Opera pia 15A 16145 Genova
Italy

MAJO CECUR
Eaton Automotive S.r.l.
Via Bicocca 28 10086 Rivarolo Canavese (TO)
Italy

Abstract: - For many decades, compromises inherent with fixed valve lift and event timing solicited engine designers to consider Variable Valve Actuator (VVA) systems as a possible option. In recent years, some relatively basic forms of VVA have been introduced into the market. VVA systems have attracted a lot of attention because of their ability to control valve events independently of crankshaft rotation, providing reduced pumping losses (work required to draw air into the cylinder) during low-load operation, and increased torque performances over a wider range than in conventional spark-ignition engines. VVA also allows control of internal exhaust gas recirculation (by controlling the valve overlap), making possible to control the NOx emissions produced during combustion.
The paper describes the EATON VVA system and the optimization process to find the best-contact components profiles and to minimize contact stresses and springs parameters. The successful optimization process, based on a Genetic Algorithm, has been performed using the ESTECO *modeFRONTIER* software. The simulation of the mathematical model, using MDI *ADAMS,* demonstrates that loads, accelerations, contact stresses at 6000rpm are lower than the maximum allowable values.

Key-Words: - VVA, simulation, optimization, ICE, valve train, lift and phase control

1 Introduction

The mechanism under study is a variable lift distribution system (Variable Valve Actuator) for internal combustion engines (ICE), developed by EATON Automotive.

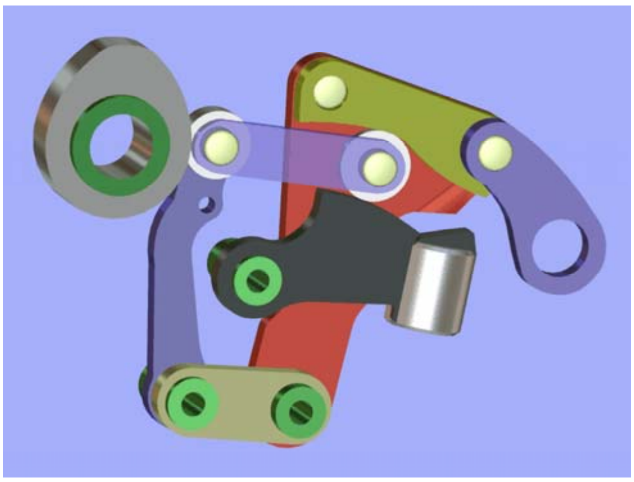

Fig. 1. EATON VVA Device

The VVA Eaton makes possible to modify the lift law both in terms of starting (and final) time of the valve event and in terms of lift amount, in a separate way and with continuity. The advantages of such a device may be summarized as follows:

- Reduced polluting emissions;
- Increased performances;
- Decreased fuel consumption;
- Elimination of the EGR devices and/or of the butterfly organs.

The essential parts of the mechanism and the ways the various controls modify the phase and the lift of the valve to obtain the expected advantages are described hereafter.
Fig. 2 shows a simplified scheme of the device.
The mechanism essentially consists of:

1. a rotating cam (indicated by its axis);
2. a roller follower;

3. a support creating a groove profile;
4. a rocker (analogous to a second follower);
5. a hydraulic lash adjuster;
6. an “elephant foot”;
7. the intake valve;
8. the phase control;
9. the lift control.

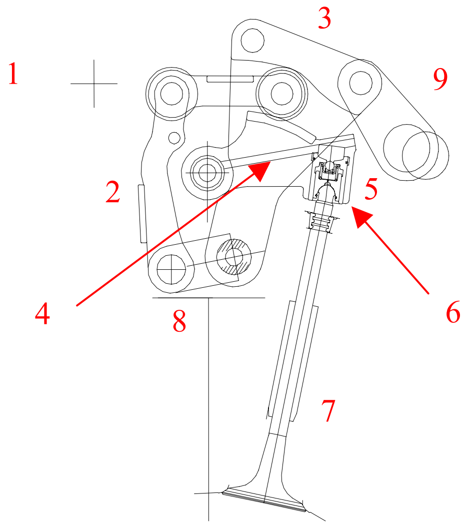

Fig. 2. Simplified model and significant parts

Fig. 3 indicates:

- Lift & Duration Control: the control of the aperture duration and of the maximum lift of the valve;
- Intake Valve;
- Timing Control: the control of the phase, i.e. the initial angle for the cam-opening event.

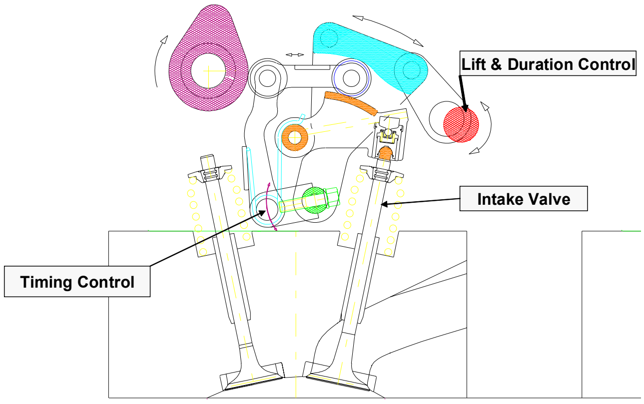

Fig. 3 Simplified diagram of the VVA EATON distribution system

In Fig. 4, the maximum lift case, it’s possible to observe that acting on the “Lift & Duration Control” (red), the profile in azure, that we will call the groove profile, is fully displaced to the left, making highly convergent the groove and permitting to the roller (blue) to fully open the valve, by acting on the rocker (orange).

In figure 5, the minimum lift case, the groove profile (in azure) is fully displaced to the right and the groove, due to the limited convergence in these conditions, make possible to the roller to open only partially (or to not open) the valve, and to produce only a minimum rotation of the rocker (in orange).

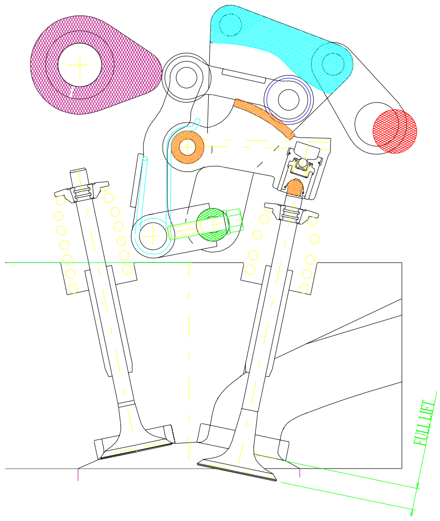

Fig. 4. Maximum lift condition

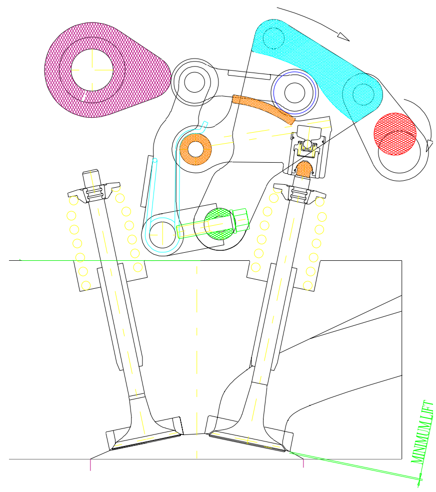

Fig. 5. Minimum lift condition

The limit case of zero lift is produced when the profiles of the rocker and of the groove are equal: in particular two concentric circle arcs, whose radii differ of the roller diameter. Fig. 6 shows the lift diagrams, which can be produced by the Eaton VVA.

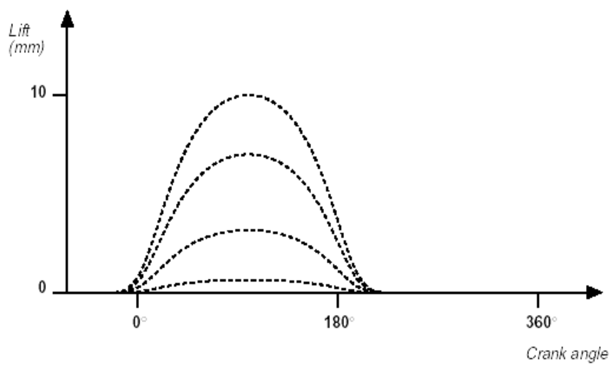

Fig. 6. The lift variation as a function of the rotation angle of the cam

Fig. 7 shows how, acting on the "Timing Control" (in green), the position of the follower with respect to the cam is displaced. In such a way it's possible to vary the starting instant of the valve opening. For a clockwise rotation of the cam, an upright displacement anticipates the lift, while a downright displacement delays it.

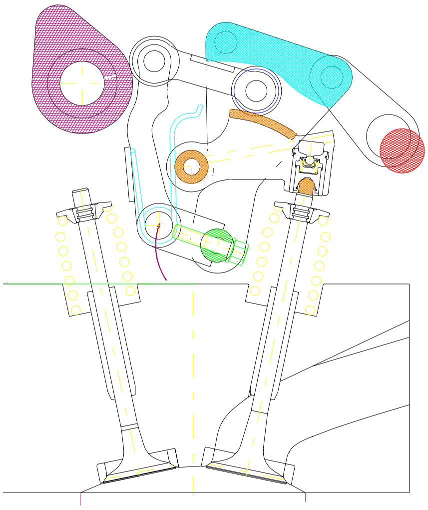

Fig. 7. Variation of the phase

Fig. 8 illustrates in detail the diagram of the lift with respect to the crank angle.

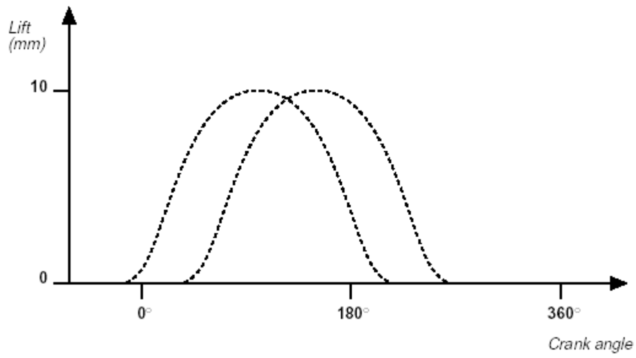

Fig. 8. Variation of the phase as a function of the rotation angle of the crank

Fig. 9 shows the variation of the phase and of the lift as a function of the cam angle.

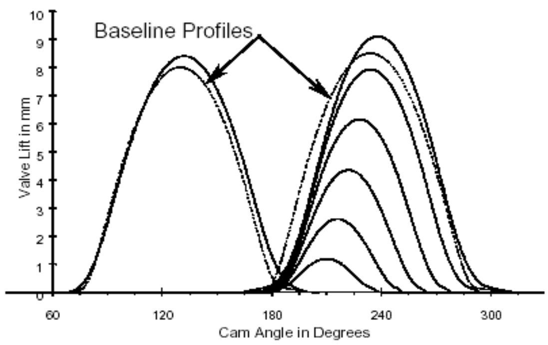

Fig. 9. Variation of the phase and of the lift as a function of the cam rotation angle

It has to be pointed out that the phase control is fully independent from the other control members, differently from the majority of the VVA and VVT present on the market.

2 Statement of the problem

The purpose of the study is to determine and to optimize

- the cam profile
- the groove profile
- the spring of the valve
- the spring of the follower

which provide the lift law (design datum), minimizing the contact stresses, in the maximum lift conditions.

2.1 Design hypotheses

Within the conditions imposed by EATON, the position of all the connection points to the frame (positions of the rotation axes) and the dimensions of the components cannot be varied, with the exception of the parts subject to contact stresses or object of this work.

2.1.1 The rollers

Since the contact between roller and rocker and between roller and groove cannot be on the same roller, three rollers must be adopted, for reasons of symmetrical distribution of loads. The assumed dimensions are: radius = 9.5mm and thickness = 10mm, for the roller-groove contact and radius = 8.5mm and thickness = 10mm for the roller-rocker contact.
Experiments done by EATON on roller followers demonstrated that a thickness greater then 10mm doesn't provide significant improvements, due to the difficulty of getting perfectly mating surfaces.

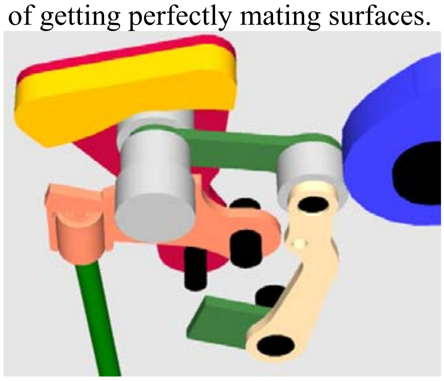

Fig. 10. Rollers

2.1.2 The rocker

Since the zero lift condition has to be provided, the three rollers must have the possibility of moving between groove profile and profile of the rocker without implying a valve lift; this is obtained with an identical profile of the two elements mentioned above. In addition, considering that the conditions at the roller/rocker interface are constant in any operation condition (lift partialization), the profiles can only be circular arches having the center at the rotation axis of the support.

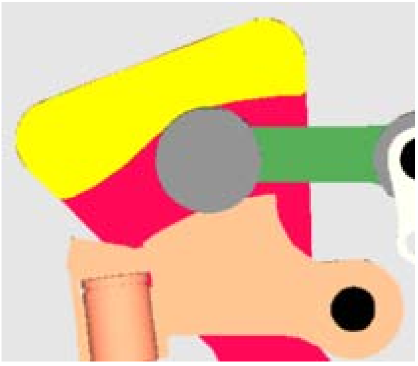

Fig. 11. The rocker

2.1.3 The groove profile

It is important to underline the strict relation between the groove profile and the cam profile in producing the imposed law of lift. These two geometries influence the dynamic characteristics of the overall mechanism. To avoid impacts of the roller on the groove profile, this last must have a radius greater than 10mm.

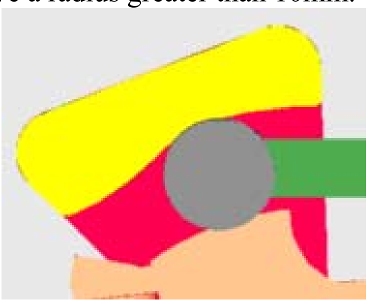

Fig. 12. The groove profile

2.1.4 The support

As far as the support is concerned, the design dimensions have to be large enough to contain the groove profile, while permitting in the meanwhile the rotation of the support around its axis. The dimensions provided by the design have been interpreted as the maximum allowable dimensions.

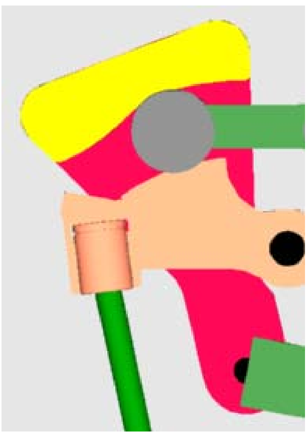

Fig. 13. The support

2.1.5 The cam profile

The cam is restricted to the shaft position specified by the project. The profile, determined through an inverse analysis, depends also on the position and on the diameter of the roller of the follower. To keep the contact stresses within acceptable values, in the case of positive curvatures normally a minimum radius greater than 14mm is adopted. For practical reasons, in the case of negative curvatures the minimum radius must be greater than 300mm.

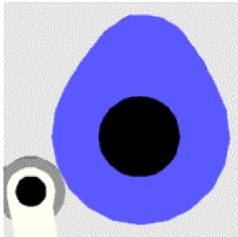

Fig. 14. The cam

3 Problem Solution

To satisfy the previous points it has been necessary to use both an optimization software (ESTECO modeFRONTIER), and a *Virtual Prototyping* software (MDI ADAMS\View) to simulate multibody models.

3.1 ADAMS \View models

A parametric model has been created, to adopt a general method of study, applicable to all the different cases.
The groove profile, the cam profile and the law of the lift univocally define the geometry of the mechanism and are fully interrelated. This arises from the way the mechanism has been created: the rigid connection between the follower roller and the triad of rollers doesn't permit to separate the effects due to the two profiles and to interpret the optimization as a synthesis of separate problems.

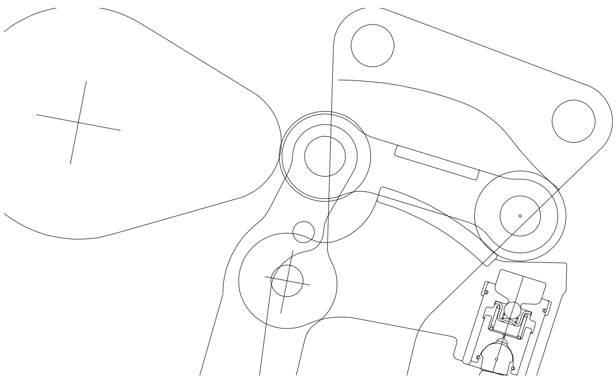

Fig. 15. A detail of the mechanism

The valve lift, in fact, depends both on the distance between the groove profile and the rocker, and on the instant the roller acts on the rocker, and therefore on the cam shape.
Since the lift law is a datum of the problem, the choice is which profile to be optimized must be considered as a

design variable and which as a simple result of the synthesis process (dependent variable). The main factor which contributed to address towards the choice of the groove profile as the independent variable was the asymmetry of the required lift law. Fig. 16 shows the lift law in the cam intervals 110°-180° and 180°-250°; the second interval has been drawn inverted to compare the curves and to show their asymmetry.

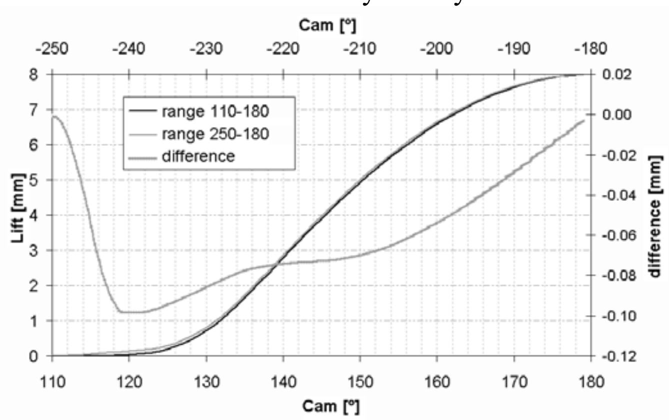

Fig. 16. Asymmetry in the lift diagram

During the 360° of the cam rotation, a roller covers in both directions the groove profile, which necessarily must be unique. The asymmetry of any lift law is created through the cam profile.

Referring to the definition of the performance index, a problem is the fact that to determine the stresses involves elevated computation times. To have very short simulation times, making possible to process an elevated number of configurations required a simplified model. The optimization has been therefore interpreted as a maximization of the geometric parameters (curvatures of the profile) and a minimization of a representative measure of the system dynamics. To that purpose the acceleration of the follower has been considered, being directly related to the components inertia and to the characteristic of the spring. For the remaining parameters, the analysis was transferred to the verification phase, after the choice of the best configuration.

The methodology just indicated focuses its attention on the determination of the geometry of the system and requires a second model, useful to evaluate the contact stresses in the verification phase.

3.2 The results of the first simulations

A detailed analysis of the results obtained from the first optimizations has shown a limit of the mechanism: the geometrical constraints of the design and, in particular, the relative position of the camshaft with respect to the follower make impossible to adopt a cam profile of a traditional type.

Under the conditions of:

- minimum positive curvature cam radius > 14mm
- minimum negative curvature cam radius > 300mm
- positive horizontal displacement of the follower roller

the significant considerations correspond to the following results:

Table 1

required measure	range	values	units
roller acceleration	0.877	1.930	[10^6 mm/s^2]
max roller displacement	0.7	3.97	[mm]

Reference values:
camshaft speed 2000 rpm
maximum valve acceleration 2.43x10^6mm/s^2

Considering all the simulations performed, the results may be grouped into three fundamental typologies:

1. negative rotations of the follower, corresponding to unacceptable operations (Fig. 17)
2. limited rotations of the follower, corresponding to groove profiles too vertical, and therefore both badly connectable with the profile corresponding to zero lift and prone to roller locking (Fig. 18)
3. elevated rotations of the follower and displacements of the roller, corresponding to cam profiles having unacceptable negative and positive curvatures (Fig. 19).

Three graphical examples of the previous typologies are reporter hereafter, showing both the computed cam profile (at the left) and the groove profile (at the right) for zero lift (B) and for the maximum lift (A).

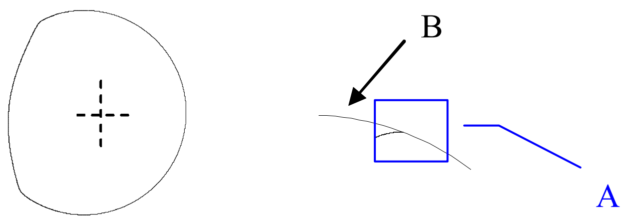

Fig. 17. Cam and groove profiles for the type 1 results

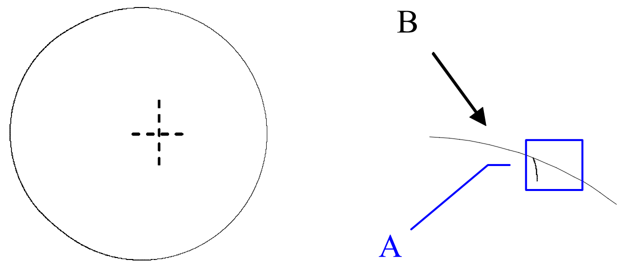

Fig. 18. Cam and groove profiles for the type2 results

Focusing the attention on Fig.19 and remembering that the valve lift depends directly on the rotation of

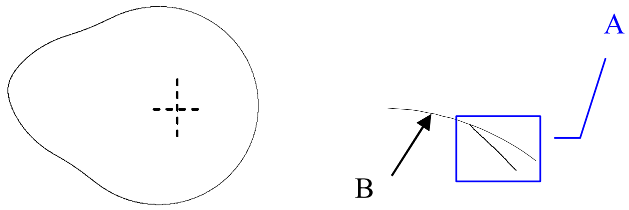

Fig. 19. Cam and groove profiles for the type 3 results

the rocker, a long path of the roller would permit a reduction of the angular accelerations and therefore of the stresses connected with the inertia forces. The figure shows that this condition is difficult to get, since it would require a maximum cam length (about 38mm) very different from the base radius (22mm) corresponding to the design specification. In this way one would obtain negative curvatures, not always acceptable, and, most of all, positive curvatures greatly exceeding the minimum imposed value (about 6mm with respect to the suggested 14mm).

In practice it's possible to attempt to limit these drawbacks by increasing the base radius, but this implies a new position of the camshaft and a greater encumbrance of the mechanism, both not allowed.

The artifact introduced to improve the profiles relative to cases (2) and (3), forces the follower to move independently and in advance with respect to the valve lift, producing an increase of the cam radius in the first rotation degrees and a short idle stroke of the roller. The profiles of the cam and of the groove obtained with and without the use of the artifact are reported hereafter.

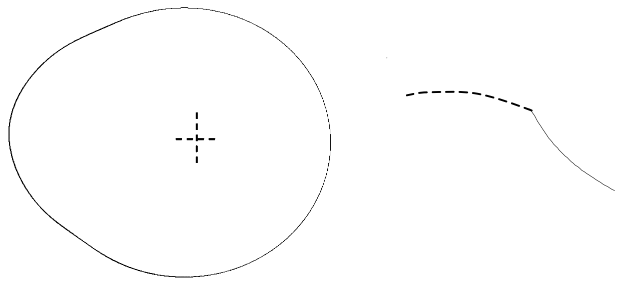

Fig. 20. Cam and groove profiles obtained without the additional rotations

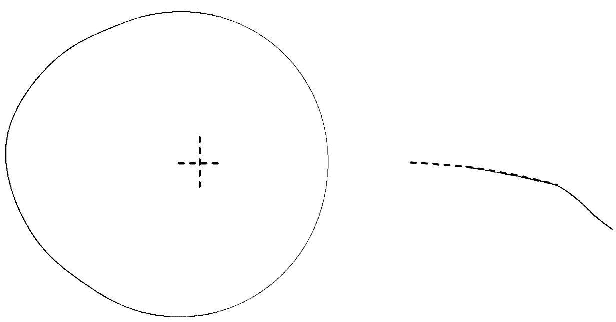

Fig. 21. Cam and groove profiles obtained with the additional rotations

In the figures 20 and 21, it's possible to observe both the previously mentioned advantages and the absence in the groove profile of the cusp arising from the connection with the zero lift interval (dashed). The effects of the support rotation and of the lift law on the profile are reported in detail in Fig.22, together with the zero lift profile (dashed).

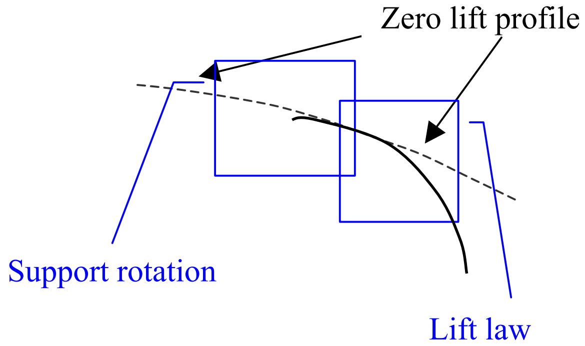

Fig. 22. Groove profile (solid line) obtained by effects superposition

The comparison with the zero lift curve shows that the support rotation cannot modify the lift law (the curves are coincident).

It's important to clarify that this procedure is only focused to the determination of the geometries and to the corresponding computation of the optimization indices. This implies that in the conditions under examination, i.e. maximum lift and zero phase variation, it's not required to act on any control foreseen (or not) by the project. The differences between some values computed with the two models are shown hereafter, for the case of eleven profiles taken as samples.

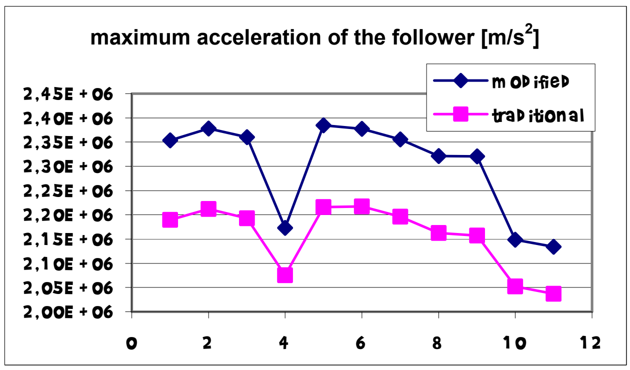

Fig. *23. Minimum positive radius of the cam [mm]*

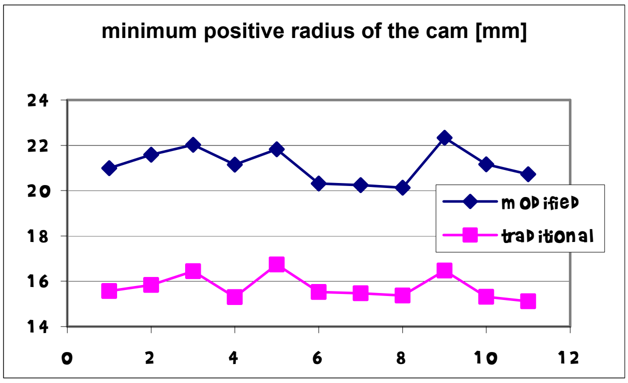

Fig. *24. Maximum acceleration of the follower [mm/s^2]*

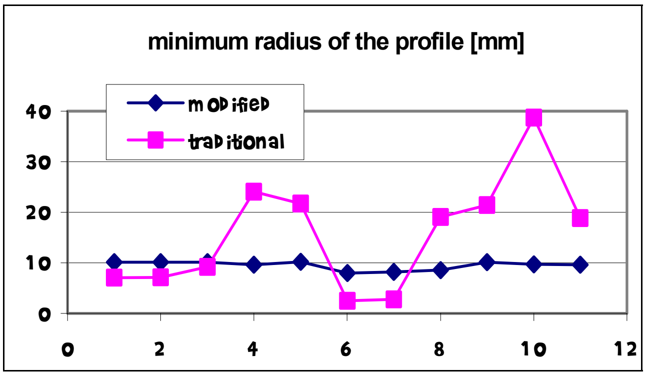

Fig. *25. Minimum radius of the groove profile [mm] for 11 groove profiles taken as samples*

Although from figures 23 e 24 one could think that the introduction of the artifact hasn't given relevant improvements, the minimum radius of the groove has to be taken into consideration (Fig. 25). This value differs in the two models since the traditional one doesn't exhibit the connection point with the zero lift profile. This value had to be evaluated and is discriminant in the choice of the profile. Also without an explicating figure, it's easy to imagine that the optimal configurations under this point of view are those having low initial slopes and comparable to those of the circle arc to be connected. This implies a relatively long groove profile, corresponding to case 3 of Fig. 19, and the corresponding difficulties.

3.3 The optimization

The optimization process used is of multi-objective type, the only valid when the need is to find the best compromise between different and conflicting objectives.

The elaboration of the process has taken about 145 hours, has tested 40960 configurations, whose 24619 unique.

The designs resulted not acceptable have been the 55% of the total, distributed as reported in Table 2.

Table 2. Simulations results

	TOTAL	
	number	%
Configurations	40960	100
not- sufficient simulation times	735	1.8
RPMIN[1] lower than 10mm	4542	11.1
RCPMIN[2] lower than 10mm	2761	6.7
RCNMIN[3] lower than 300mm	2843	6.9
significant	**18249**	**44.5**

Reference values:
cam velocity: 2000 rpm

Considering only the results whose values of ACCMAX[4] are lower than the valve acceleration (2.43x10^{6}mm/s^2), we get:

significant configurations	**17594**	**43.2**

The values computed during the simulations in general exhibit a large range of variability, with the exception of the geometric parameters. E.g. RPMIN varies from 10mm to 11.3mm and the cam profiles having negative curvature are very few (less than 2‰), although RCNMIN varies from 580mm to ∞.

Table 3 summarizes the ranges of variability of the significant configurations.

Table 3. Extreme values

	units	min	max
ACCMAX	[10^{6}mm/s^2]	1.22	2.43
RPMIN	[mm]	10	11.32
RCPMIN	[mm]	14	24.7
RCNMIN	[mm]	580	∞

The best results of the optimization process have been obtained with reference to ACCMAX, since the significant configurations have converged around its minimum values. The Frequency plot of Fig. 26 gives the average value 1.6x10^{6}mm/s^2, a low value if compared with the maximum acceleration of the valve (2.43x10^{6}mm/s^2), but the most elevated peaks are in correspondence of the lower limit.

[1] Minimum value of the radium of curvature of the groove profile: RPMIN
[2] Minimum value of the radium of positive curvature of the cam profile: RCPMIN
[3] Minimum value of the radium of negative curvature of the cam profile: RCNMIN
[4] Maximum value of the acceleration of the follower: ACCMAX

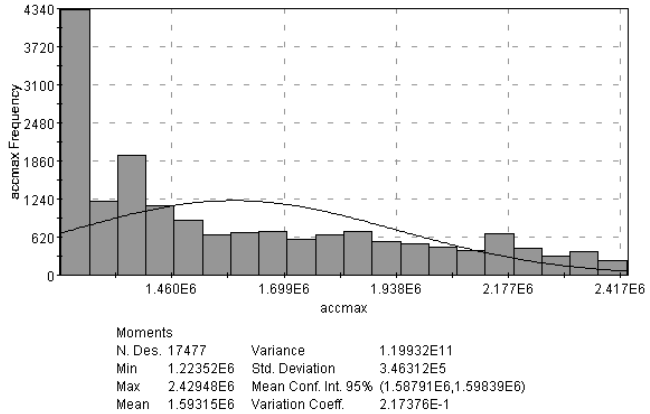

Fig. 26. Frequency plot of ACCMAX [mm/s^2]

The values of RPMIN are in conflict with the goals of the optimization (Fig. 27) since they thicken around the minimum values of the parameter (average value = 10.3mm).

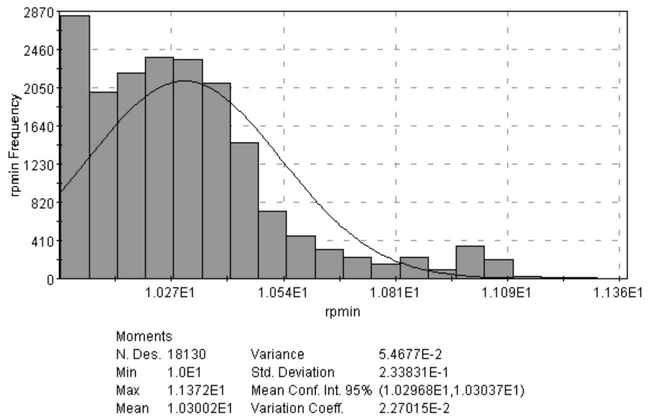

Fig. 27. Frequency plot of RPMIN [mm]

This suggests, in addition to the complexity of the optimization, the fact that the different objectives bring to highly conflicting solutions.

As far as RCPMIN is concerned, optimization didn't move towards the upper extreme of the definition interval; from the values reported in Fig. 28 the average results to be a bit lower than 20mm.

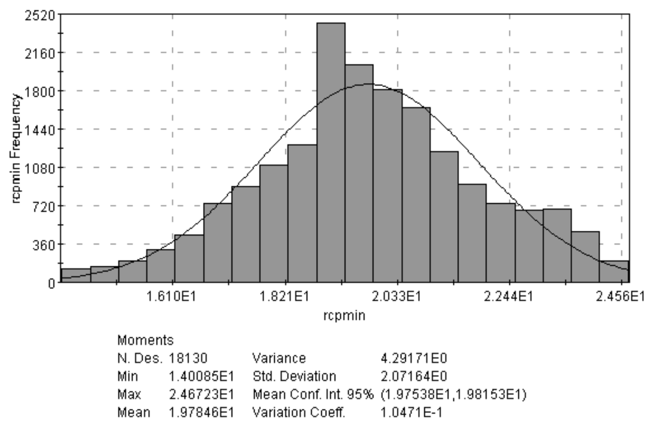

Fig. 28. Frequency plot of RCPMIN [mm]

From a comparison of the objectives interesting facts come into evidence; between them the confirmation that high values of RCPMIN correspond to low values of RPMIN (Fig. 29)

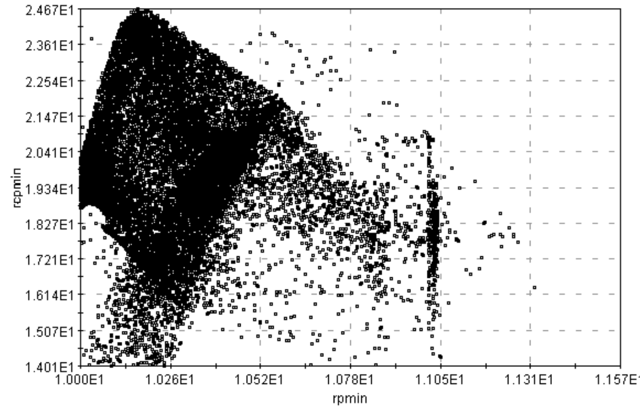

Fig. 29. Plot of RPMIN [mm] versus RCPMIN [mm]

From the comparison of the maximum acceleration of the follower with the radii of curvature, it becomes apparent that to the best values of ACCMAX correspond minimum values of RPMIN (Fig. 30) and maximum values of RCPMIN (Fig. 31); this in practice cuts any possibility of choice of a configuration without the help of the software.

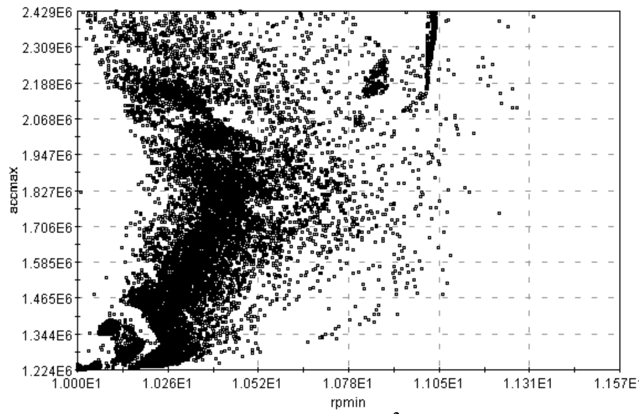

Fig. 30. Plot of ACCMAX [mm/s^2] versus RPMIN [mm]

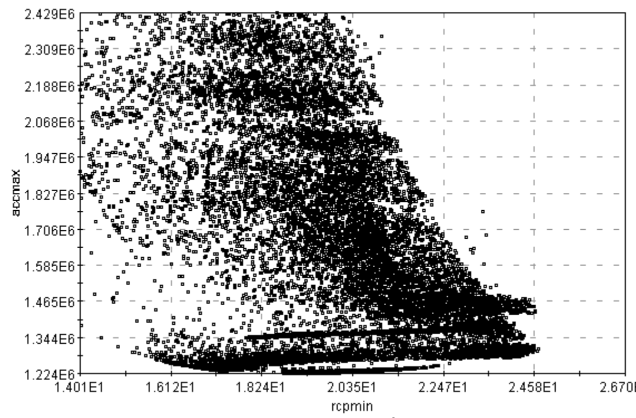

Fig. 31. Plot of ACCMAX [mm/s^2] versus RCPMIN [mm]

In addition, it has to be observed that, although the variation of RPMIN is extremely small (0.13mm), this is not the case of the variation of ACCMAX, ranging in all the interval of definition (about 1.23x10^{6}mm/s^2).

3.3.1 The Pareto Set

modeFRONTIER permits to look for the best solutions by determining, in the mostly effective possible way, the Pareto Set, i.e. the set of alternatives such that it's impossible to approach more an objective without increasing the distance from the other. modeFRONTIER identified 1087 of 24619 configurations (the 4.5%) between which to perform the final choice. The values so computed have the ranges of variability summarized in Table 4.

Table 4. Comparison between the extreme values of the Pareto Set and of the optimization

		PARETO SET	
	units	min	max
Accmax	[10^{6}mm/s^2]	1.22	1.27
Rpmin	[mm]	10	10.4
Rcpmin	[mm]	15.8	20.4
Rcnmin	[mm]	∞	∞

With reference to the global extreme, a general reduction is apparent for the upper limits, with a clear improvement of the acceleration of the follower, whose maximum value has been practically halved (1.27x10^6 instead of 2.43x10^{6}mm/s^2). This improvement is not present in RCPMIN and RPMIN, with a significant reduction of the upper limits (respectively 20.4 and 10.4 instead of 24.7 and 11.3mm).
Comparing the acceleration of the follower with both the geometrical parameters, again the opposite trends come into evidence, as shown in Fig.32.

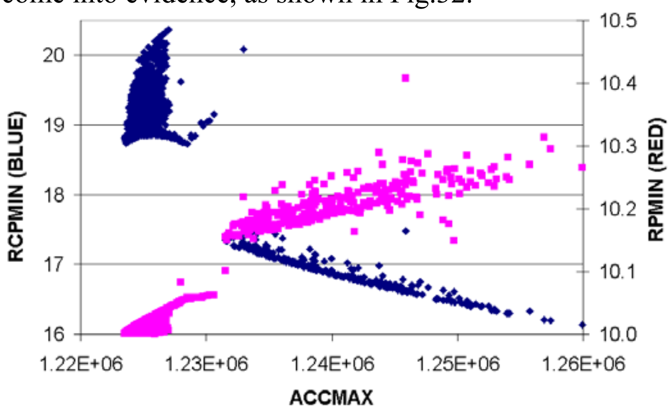

Fig. 32. Comparison between ACCMAX [mm/s^2] and the geometrical parameters [mm] of the Pareto Set

3.3 The MCDM

The Multi Criteria Decision Making Tools made available by the software, elaborate the data provided by the Pareto Set into a transfer function giving an estimate (*Range Value*) of the designs in a global vision of the problem. The contributions of each performance index (*Attribute*) are computed through *Utility Functions,* reported in Fig.33, as a function of each objective (*Attribute Range*).

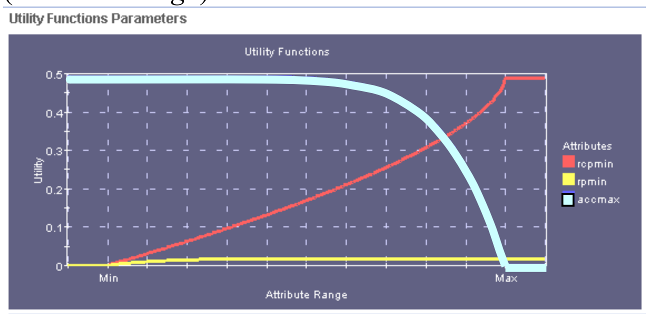

Fig. 33. Utility Function Parameter for each performance index

The functions in the figure are determined by modeFRONTIER through genetic algorithms and are clearly non-linear. The maximum values (weight) for each function and some characteristics of the curves have been summarized in Table 5.

Table 5. Reference values for the transfer function

value	attribute range		objective	type	weight
	min	max			
rcpmin	15.76	20.36	max	non linear	0.4895
rpmin	10.00	10.41	max	non linear	0.0180
Accmax (x10^6)	1.22	1.27	min	non linear	0.4923

Table 6. Configurations having the higher Rank Value

<Id>	Rcpmin [mm]	Rpmin [mm]	Accmax [10^{6}mm/S^2]	**Rank Value**
19267	20.37	10.01	1,2270	0.9837
6460	20.36	10.01	1,2269	0.9730
29816	20.31	10.01	1,2265	0.9504
28749	20.31	10.00	1,2266	0.9496
31293	20.30	10.01	1,2265	0.9465
35816	20.26	10.00	1,2262	0.9338
33052	20.24	10.01	1,2262	0.9306
35219	20.23	10.00	1,2260	0.9254
26566	20.20	10.01	1,2263	0.9215
38686	20.17	10.02	1,2268	0.9160
6556	20.15	10.01	1,2260	0.9093
36906	20.13	10.01	1,2259	0.9042
27426	**20.09**	**10.21**	**1,2329**	**0.9002**
29829	20.11	10.00	1,2254	0.8991

The transfer function, i.e. the sum of the contribution computed through the *Utility Functions*, makes possible to range the configurations of the Pareto Set as a function of the computed value (*Rank Value*).
Table 6 reports some of the designs that have been considered to be the best by the algorithm.
The table reports both the number of the simulation (*ID*) and the values of the objectives.
Between the configurations in the list, only the 27426 has a quite high value of RPMIN: it has been chosen as the preliminary design solution, although the value of ACCMAX is slightly more elevated. The configuration has produced the profiles reported in the figures 34 and 35.

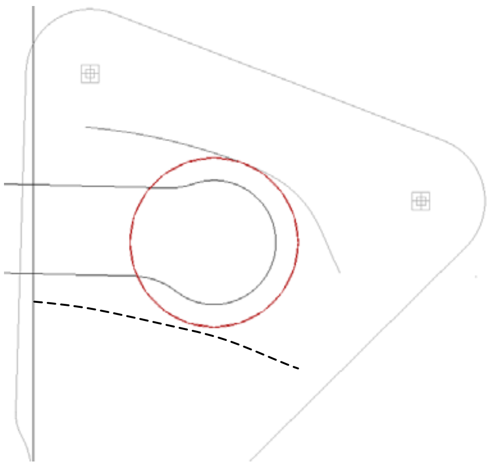

Fig. 34. Groove profile and roller

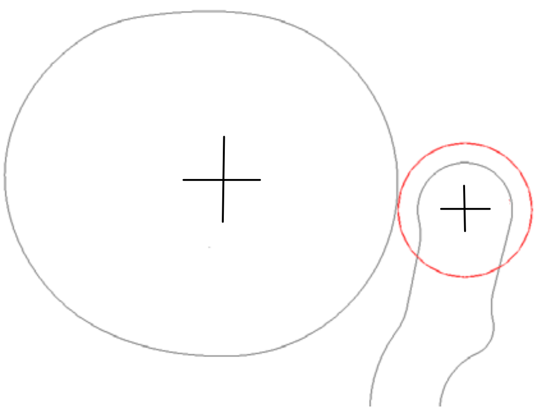

Fig. 35. Cam profile and roller

Figures 36 and 37 show the curvatures of the profiles.

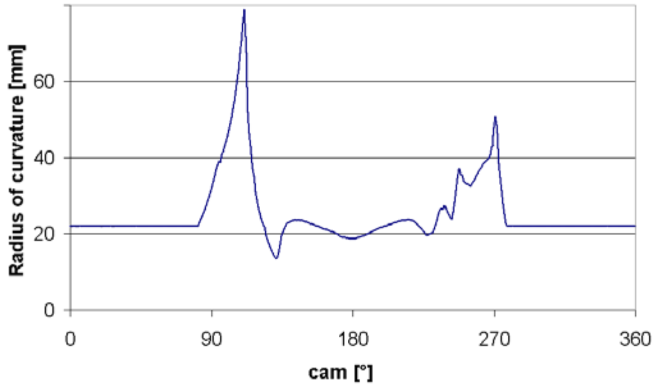

Fig. 36. Radii of curvature of the cam profile

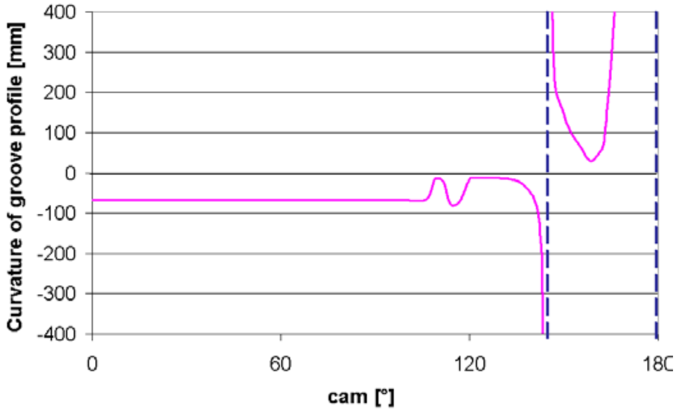

Fig. 37. Radii of curvature of the groove profile

Fig. 37 exhibit a flexure point around 140° of the cam angle and reports the vertical asymptotes (dashed lines; straight lines, radius $\rightarrow \infty$).

4 Verification

In comparison with the approach followed above, the model used to evaluate the stresses is much more accurate and adherent to the real mechanism; in addition it contains the elastic elements necessary to keep the members in contact. There are two springs, one acting on the follower, the other axially on the valve (Fig.38).
The project prescribes to simulate, for the spring 1, a longitudinal element placed at about 60% of the follower height and having the characteristics reported in the figure. The spring 2, analogous to those adopted in the traditional distribution mechanisms, is coaxial with the valve. The characteristics indicated in the figure are about 20% lower with respect to the maximum usually adopted.
The checks were performed for the time interval where the valve lift has a non-zero value (Fig.39). This was because in model used the seat of the valve was not simulated and therefore the stresses were not zero in the remaining interval, a fact not in agreement with the real behavior of the mechanism.

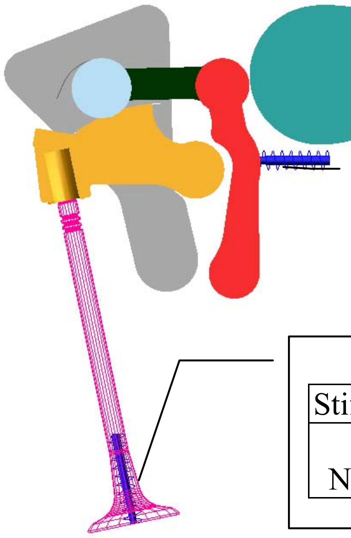

Spring 1	
Stiffness	Preload
12 N/mm	120 N

Spring 2	
Stiffness	Preload
20 N/mm	200 N

Fig. 38. Characteristics of the springs present in the model

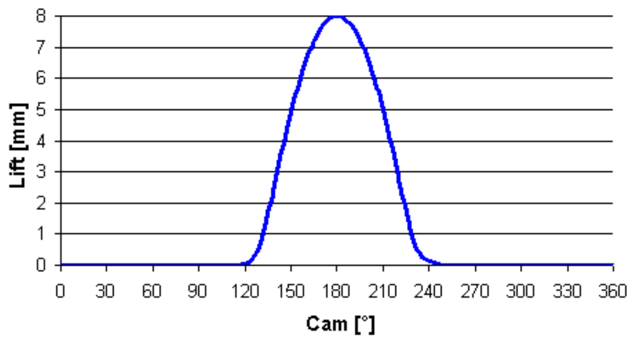

Fig. 39.The lift diagram provided by the project

4.1 Verification of the lift law

The values of the lift are computed as displacements of the center of mass of the valve along the axis of the valve itself. The EATON specifications consider a maximum difference of 0.05mm between the design value and the true one. Fig. 40 shows that such a tolerance has been respected, with a maximum difference of about 0.045mm.

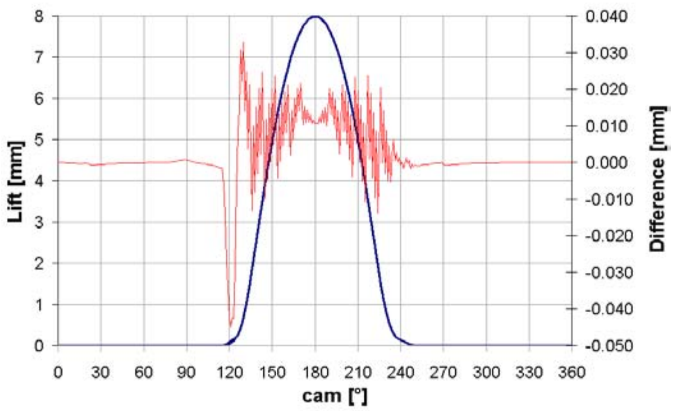

Fig. 40. Plot of the valve lift obtained by simulation (blue) e difference with respect to the design values (red)

4.2 Verification of the stresses at the cam-roller interface

The analysis of the maximum allowable solicitations, computed through the Hertz theory and reported in Fig. 41, shows with respect to the simulation values a minimum difference of about 180N at 227°of the cam angle.

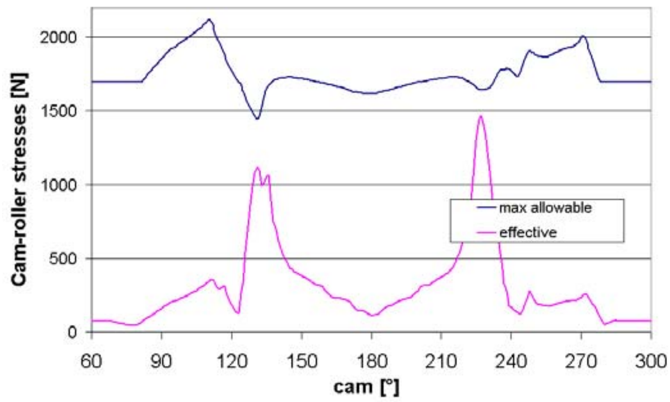

Fig. 41. Maximum allowable forces (blue) and computed forces (red)

4.3 Verification of the stresses at the rocker-roller interface

The maximum value of the solicitations computed by ADAMS is 1660N at 0.0071s (128° of cam angle) and, as it can be seen in Fig.42, in the worst case there is a difference of about 350N with respect to the maximum allowable (2000N).

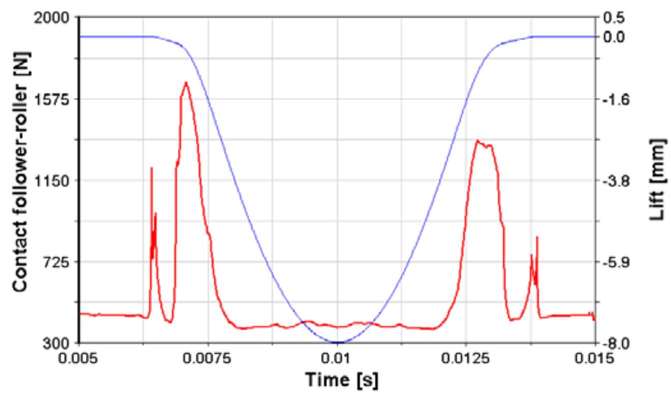

Fig. 42. The maximum allowable forces (green), the effective forces (red) and the valve lift (blue)

4.4 Verification of the stresses at the support-roller interface

The heaviest condition, corresponding to the point indicated in Fig. 43 and identified by a radius of positive curvature of 30.5mm, is found at 155° of cam angle (and also at 205°) with the high value of about 3500N.

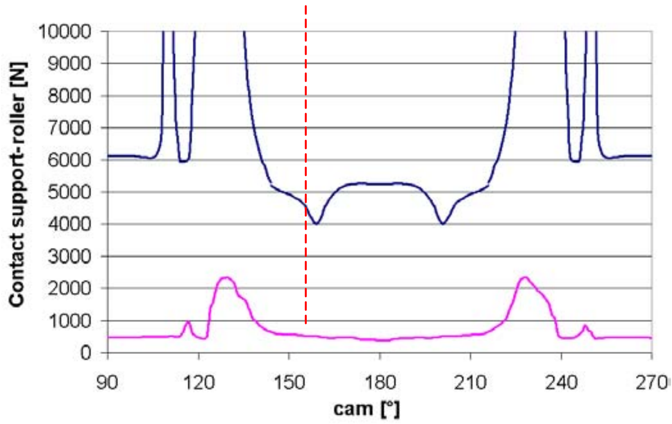

Fig. 43. The contact forces at the support-roller interface (red), the maximum allowable loads (blue), and the most critical point (dashed line)

4.4 The springs

The springs tentatively chosen at the beginning of the verification process (Fig. 38) have optimally performed with respect to the cam speed, keeping in contact the profiles.

By carefully studying the mechanism it can be observed that the two springs collaborate in keeping the members in contact; this gives a greater freedom in the choice of the elastic elements. In fact the characteristics of a spring can be increased in favor of a decrease in the other and vice versa, according to an approximately linear relationship.

By simulation the behaviors of different configurations, the results summarized in Fig.44 have been obtained: ordinates and abscissas report the values of stiffness and preload [5], respectively of spring 1 and spring 2.

The lines in red correspond to the maximum rotation speeds of the cam simulated with a positive result. In particular the elastic elements are able to assure the contact of the members of the mechanism, with stresses lower than the maximum allowable, with the exception of the 7000 rpm configuration. With the exception of this last case, in fact, the maximum solicitations differ very little from simulation to simulation.

4 Conclusion

The study on the VVA EATON device used the virtual prototypation techniques to create a mathematical model of the mechanism to simulate its performances. The device has been completed with the missing parts, the profiles of the cam and of the groove, which were the object of an optimization procedure. In addition, simulations have been performed to check that the innovating distribution system and in particular its contact elements were such to satisfy the exigencies of a wide choice of engine models.

The model and the simulations have been performed in MDI ADAMS, the well-known software for mechanical systems simulation.

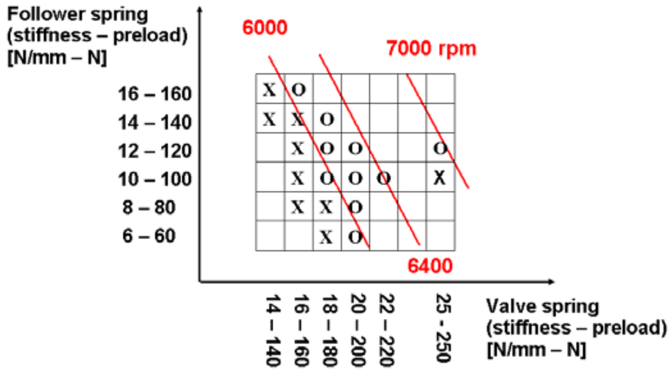

Fig. 44. Configurations simulated with positive (O) and with negative (X) results

The initial data were the basic dimensions of the mechanism and the objectives to be fulfilled, consisting in the search of the best profiles for the cam and for the groove to limit the contact stresses and of the characteristics of the springs. In addition it was required to be able to resist to the solicitations of the high speeds of the engine.

Given the nature of the contacts, reference has been made to the Hertz theory; limits have been imposed on the geometries to be optimized, on the basis of the EATON experience in the automotive field.

The presence of such limits determined the choice of the geometrical parameters as performance indices of the model, jointly with a parameter representing the stresses under examination. The refinement of the model and of the method of creating the profiles and, not least, the use of the procedures of the optimization software ESTECO modeFRONTIER have made possible to test more than 40˙000 different profiles.

Table 7. Values of the performance indices of the Pareto Set and their limitations

performance index	units	limits	min value	max value
RPMIN	[mm]	> 10	10	10.4
RCPMIN	[mm]	> 14	15.8	20.4
RCNMIN	[mm]	> 300	∞	∞
ACCMAX	[mm/s^2]	< 2.43×10^6	1.22×10^6	1.27×10^6

From the point of view of the results, the techniques based on genetic algorithms have permitted to identify

[5] The values of the ordinates and of the abscissas have been determined by considering approximately a factor 10 between stiffness and preload.

1087 candidates to be considered for the choice. These candidates, whose performance indices are summarized in Table 7, with the above mentioned limitations, constitute the Pareto Set, i.e. the design set where it's impossible to approach further an objective without increasing the distance from the other.

To find the best solution within the Pareto Set, multi-criteria decision techniques have been used; they have pinpointed the profile having the following characteristics:

PERFORMANCE INDEX	VALUE	
RPMIN	10.21	mm
RCPMIN	20.09	mm
RCNMIN	∞	mm
ACCMAX	1.233×10^6	mm/s^2

The verification of the stresses, the last step of this study, demonstrated the validity of the process and the possibility of using the mechanisms in engines steadily reaching 6000 rpm.

The results reported in the table show a large difference between the maximum allowable stresses and the effective ones in the contact between the support and the roller.

Table 8. Solicitations: maximum effective, maximum allowable and minimum difference[6]

contact surfaces	maximum effective solicitation	maximum allowable solicitation	minimum difference
cam/ roller	1470N	1650N	180N[7]
rocker/roller	1660N	2000N	340N[8]
support/ roller	2341N	4000N	3550N[9]

This difference suggests the possibility to reduce the contact surfaces, improving the compactness and lowering the inertias.

Concerning the springs, an approximate inverse proportionality has been detected between the characteristics of the elastic elements.

In addition, the critical point has been detected to be the cam/follower subsystem, having the minimum difference between the maximum allowable stresses and those computed during the simulation.

[6] The values of the difference are the minimum in the interval of the analysis, i.e. during the 360° of rotation of the cam

[7] The datum refers to 225°of cam angle

[8] The datum refers to 130° of cam angle

[9] The datum refers to 155°and 205°of cam angle

References

[1] J.B.Heywood, *"Internal Combustion Engine Foundamentals"* Mc Graw-Hill, 1988

[2] H.P.Lenz, K.Wichart and D.Gruden, *"Variable Valve Timing - A Possibility to control Engine Load without Throttle"* SAE Paper 880288, 1988

[3] D.N.Assanis and B.K.Bolton, "*Variable Valve Timing Strategies for Optimum Engine Performance and Fuel Economy*" Proceedings Energy Sources Technology Conference and Exhibition, Detroit, 1994

[4] M.Pischinger, "*A New Opening*" Engine Technology International, 2000 Annual Review

[5] R.Pierik, "*The Application and Engine Performance Benefits of a Mechanical Variable Valve Actuation System*" 7th Aachen Kolloquium Fahrzeug- und Motorentechnik, Aachen, Germany, 1998

[6] R.Pierik and J.F.Burkhard, *"Design and Development of a Mechanical Variable Valve Actuation System"* SAE 2000 World Congress, Detroit, Michigan, 2000

[7] S.H.Richardson, Ahmar Ghauri, C.J.E.Nightingale, *"Variation of Both Simmetric and Asimmetric Valve Events on a 4-Valve SI Engine and the Effects on Emissions and Fuel Economy"* SAE Paper 2000-01-1222, 2000

[8] D.Goldberg. *Genetic Algorithms in search, optimization and machine learning*. Reading, Mass., Addison-Wesley, 1989

[9] K.Deb. *Multi-objective Genetic Algorithms: Problem Difficulties and Construction of Test Problems.* Technical Report CI-49/98, University of Dortmund, October 1998

[10] J.H.Holland. *Adaption in Natural and Artificial Systems*. MI. University of Michigan Press, 1975

[11] ES.TE.CO. *modeFRONTIER User Manual.*, 2002

[12] R.Janssen, M.Herwijnen, *"DEFINITE, a System to Support Decisions on a FINITE Set of Alternatives"*. Kluwer, Dordrecht/Boston/London,1994.

[13] F.A.Lootsma, *"Multi-criteria Decision Analysis via Ratio and Difference Judgement"*. Kluwer, Dordrecht/Boston/London,1999.

[14] R.H.Myers and D.C.Montgomery. *"Response Surface Methodology: process and product optimization using designed experiments"*, Wiley, 1995.

[15] MDI. *Building your model in ADAMS\View*,. 2002

[16] MDI. *ADAMS\Solver User Guide*, 2002

[17] MDI. *Using ADAMS\PostProcessor*, 2002

[18] N.Diaconu, L.Tomescu, I.Crudu, *"Theoretical Model for Estimating the Stress Distribution within the superficial layer, for two cylinders contact"* Annals of University of Galati, VIII, ISSN 1221-4590, 2002.